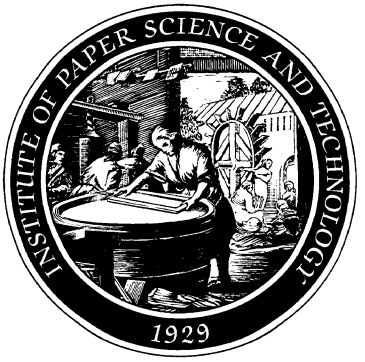

Institute of Paper Science and Technology
Atlanta, Georgia

IPST Technical Paper Series Number 866

Gas Flow Regime Changes in a Bubble Column Filled with a Fibre Suspension

T.J. Heindel

June 2000

Submitted to
The Canadian Journal of Chemical Engineering

INSTITUTE OF PAPER SCIENCE AND TECHNOLOGY
PURPOSE AND MISSIONS

The Institute of Paper Science and Technology is an independent graduate school, research organization, and information center for science and technology mainly concerned with manufacture and uses of pulp, paper, paperboard, and other forest products and byproducts. Established in 1929 as the Institute of Paper Chemistry, the Institute provides research and information services to the wood, fiber, and allied industries in a unique partnership between education and business. The Institute is supported by 52 North American companies. The purpose of the Institute is fulfilled through four missions, which are:

- to provide a multidisciplinary graduate education to students who advance the science and technology of the industry and who rise into leadership positions within the industry;
- to conduct and foster research that creates knowledge to satisfy the technological needs of the industry;
- to provide the information, expertise, and interactive learning that enables customers to improve job knowledge and business performance;
- to aggressively seek out technological opportunities and facilitate the transfer and implementation of those technologies in collaboration with industry partners.

ACCREDITATION

The Institute of Paper Science and Technology is accredited by the Commission on Colleges of the Southern Association of Colleges and Schools to award the Master of Science and Doctor of Philosophy degrees.

NOTICE AND DISCLAIMER

The Institute of Paper Science and Technology (IPST) has provided a high standard of professional service and has put forth its best efforts within the time and funds available for this project. The information and conclusions are advisory and are intended only for internal use by any company who may receive this report. Each company must decide for itself the best approach to solving any problems it may have and how, or whether, this reported information should be considered in its approach.

IPST does not recommend particular products, procedures, materials, or service. These are included only in the interest of completeness within a laboratory context and budgetary constraint. Actual products, materials, and services used may differ and are peculiar to the operations of each company.

In no event shall IPST or its employees and agents have any obligation or liability for damages including, but not limited to, consequential damages arising out of or in connection with any company's use of or inability to use the reported information. IPST provides no warranty or guaranty of results.

GAS FLOW REGIME CHANGES IN A BUBBLE COLUMN FILLED WITH A FIBRE SUSPENSION

Theodore J. Heindel
Institute of Paper Science and Technology
500 10th Street NW
Atlanta, GA 30318-5794
ted.heindel@ipst.edu

ABSTRACT

Gas flow characteristics in opaque fibre suspensions have been captured on film using a stop-motion x-ray imaging technique called flash x-ray radiography (FXR). Gas flows in a bubble column filled with various cellulose fibre suspensions from 0% (an air-water system) to 5% by mass have been observed. The gas flow regime changes from vortical to churn-turbulent as the fibre concentration increases for a fixed superficial gas velocity. Two new gas flow regimes, identified as surge churn-turbulent and discrete channel flow, have also been recorded at high fibre concentrations.

KEYWORDS

bubble column; fibre suspension; flow visualization; gas flow regimes; x-rays

INTRODUCTION

Bubble columns are commonly used in many process industries to enhance heat and mass transfer between a liquid and gas phase, to promote chemical or biochemical reactions between phases, or to separate one constituent from another. They are typically operated in one of two generally identified flow regimes. In the bubbly or homogeneous flow regime, gas bubbles are typically small and uniform in size, and rise in a homogeneous dispersion through a continuous liquid phase with minor interactions (i.e., coalescence) between bubbles. The churn-turbulent or

heterogeneous flow regime is characterized by a heterogeneous flow of small bubbles and rather large bubbles that form by the coalescence of small and/or large bubbles. One particular property of these large bubbles is that they undergo frequent coalescence and breakup (De Swart et al., 1996; Tsuchiya et al., 1996). The transition region between bubbly flow, also called dispersed bubble flow by Chen et al. (1994), and fully churn-turbulent flow has been characterized as vortical flow for two-dimensional bubble columns (Tzeng et al., 1993) and vortical-spiral flow for three-dimensional bubble columns (Chen et al., 1994).

These flow regimes are easily identified by optical visualization techniques in a transparent air-water system. When the system is translucent, opaque, or optical visualization is limited (common in many process industries), selected probes may be inserted to measure gas holdup (Hewitt, 1982; Saxena et al., 1988). Flow regime identification is obtained from this information by observing the gas holdup dependence on superficial gas velocity (Zahradnik et al., 1997; Sarrafi et al., 1999). The recording of bubble frequency and size has also been used to identify gas flow regimes in multiphase systems (Zhang et al., 1997). Chaos theory has also recently been used to identify the transition from homogeneous to heterogeneous flow conditions (Letzel et al., 1997).

Radiation techniques can also be used to measure gas holdup (Hewitt, 1978; Lindsay et al., 1995; Kumar et al., 1997; Shollenberger et al., 1997) and visualize gas flows in multiphase systems (Bennett et al., 1965; Hewitt and Roberts, 1969; Rowe and Partridge, 1965; Heindel and Monefeldt, 1998). One radiation technique that can be used to visualize gas flow structures in opaque multiphase systems involves stop-motion x-rays, called flash x-ray radiography (FXR). This is a process where an intense burst of x-ray radiation is produced for a fraction of a second to record dynamic events on film that cannot be captured by conventional photography (Jamet

and Thomer, 1976; Cartz, 1995). FXR has recently been used to observed gas flow patterns (Heindel and Monefeldt, 1997, 1998) and measure bubble size (Heindel, 1999; Heindel and Garner, 1999) in cellulose fibre suspensions with fibre concentrations up to 1.5% by mass. These previous results have shown that the presence of fibres, even at relatively low mass fractions, promoted large bubble formation and churn-turbulent flow conditions. Additionally, by focusing on only small bubbles, defined as those with equivalent diameters less than 12 mm, Heindel and Garner (1999) have shown that small bubbles in fibre suspensions can be characterized by a single lognormal distribution. However, this conclusion is applicable only for fibre consistencies up to 1.5% by mass.

In this technical note, gas flows in cellulose fibre suspensions at fibre concentrations as high as 5% by mass are visualized with FXR for the first time. Qualitative observations of these flow conditions are described in detail and two new gas flow regimes are identified in these suspensions.

EXPERIMENTAL METHODS

Figure 1 is a schematic representation of the experimental setup used in this study. The bubble column was 1 m tall with a rectangular cross section of 20 cm × 2 cm, and was constructed with face panes of 6.35 mm clear acrylic stock. Compressed and filtered air was injected into the base of the column through a sintered bronze sparger with a nominal pore diameter of 40 μm. This was attached to the end of a flexible air line and placed on the bottom of the column. The air line was positioned near the column wall such that it did not interrupt the bulk bubble flow patterns, and the sparger was centrally located on the column floor. For fibre concentrations greater than 2%, the flexible air line was placed within a small diameter pipe to keep the backmixed flow from moving the line into the center of the column, which disrupted the

central location of the sparger. A volumetric air flow rate of 2 liters per minute was fixed for all experiments. This corresponded to a constant superficial gas velocity of 0.83 cm/s. As described, the bubble column can be likened to a graduated cylinder with a rectangular cross section. Air passed through it, but no bulk exchange of liquid occurred (i.e., the superficial liquid velocity was zero).

The x-ray unit was a 300 keV HP 43733A flash x-ray system (Maxwell Physics International, San Leandro, CA, USA), which generated a 30 nanosecond x-ray pulse. The fast x-ray pulse provided stop-motion x-rays of gas bubbles rising through the fibre suspension. Complete details of the FXR procedures have been outlined by Heindel and Monefeldt (1998). A single 20 cm × 25.2 cm x-ray negative was exposed during each discharge of the x-ray unit.

The systems of interest were composed of deionized water with or without cellulose fibre (i.e., repulped unprinted chemical fibre) at ambient temperature (~22°C). The cellulose fibre had a length-weighted average length of 1.3 mm and a coarseness (fibre mass per unit length) of 0.13 mg/m. The cellulose fibre was reslushed at a fibre concentration of approximately 11% by mass using a high consistency pulper. The fibre concentrations, C, imaged in this study ranged from $C = 0$ (corresponding to an air-water system) to $C = 5\%$ by mass, in 0.5% increments. The various fibre concentrations were prepared by diluting samples of the high concentration stock with deionized water. The surface tension of a fibre suspension filtrate sample was measured to be approximately 63 dynes/cm. No additional surface active agents were introduced into the system, except for those that may be associated with the added cellulose fibre. Therefore, the observations presented here are for "clean" fibre suspensions. However, as recently noted by Janse et al. (1999), surface active agents can have a significant effect on the gas flow characteristics in fibre suspensions. This will be a topic for future FXR studies.

The bubble column was charged by filling it from the top with 3.2 L of the desired fibre slurry, corresponding to a column fluid height of 80 cm. This allowed for fluid expansion in the bubble column during air injection. After the air was turned on, a waiting period of approximately 10-15 minutes allowed the flow to reach quasi-steady-state conditions, at which time x-rays were taken at one of four column positions identified in Fig. 1.

RESULTS

One column location (position 2) will be used to visually summarize the effect cellulose fibre concentration has on the gas flow structures in fibre suspensions with $C \leq 5\%$. Column composite images at selected fibre concentrations will then be presented to provide an overall qualitative picture of the gas flow structures in the entire bubble column.

Figure 2 shows representative FXR images of position 2, encompassing a column height of approximately 25-45 cm from the column base. For all fibre concentrations, the superficial gas velocity is fixed at 0.83 cm/s. The dark regions represent air bubbles, and the air line is apparent on the left-hand side of each radiograph. The actual x-ray image is 20 cm × 25.2 cm, with approximately 2.5 cm of film extending beyond each side of the bubble column. These regions include lead position indicators (affixed to the column exterior) and radiograph identification labels, and have been digitally removed from each image to enhance clarity. Therefore, each image in Fig. 2 encompasses the entire column width of 20 cm and a column height of 20 cm. Additionally, bubble diameters on the order of 1 mm can be resolved on the actual radiographs, but details this fine are lost when the entire image is reduced for presentation in Fig. 2. However, all observations are based on the actual images.

An air-water system (C = 0%) is shown as a reference condition in Fig. 2a. When no fibres are present, the majority of the bubbles are uniform in size and well dispersed throughout the bubble column. Some bubbles form groupings and appear as large bubbles in the digitized image, but they are actually individual bubbles that rise as a group. The bulk of the bubbles rise in a serpentine pattern that oscillates from one side of the column to the other. Backmixing is also visually observed, but difficult to capture during the stop-motion FXR exposure. The flow regime for C = 0% would be considered vortical flow (Tzeng et al., 1993; Chen et al., 1994).

Figure 2b shows that when as little as 0.5% by mass of cellulose fibre is added to the bubble column, the bubble size and shape change considerably. Many small bubbles are still present, but are fewer in number due to the addition of extremely large bubbles. These observations were also made by Reese et al. (1996) and Heindel and Garner (1999). The large bubbles are generally spherical-capped, but variations are observed. Some of the large bubbles encompass more than 10% of the column width of 20 cm. This would make them large enough to span the entire column depth of 2 cm. The large bubbles rise in a serpentine pattern, undergo considerable coalescence and breakup, and entrain smaller bubbles in their wake as they rise. Backmixing is also very evident during visual inspection. Since considerable bubble coalescence and breakup are visually observed, the flow regime for C = 0.5% would be considered churn-turbulent (Tzeng et al., 1993). Therefore, the presence of 0.5% by mass of cellulose fibre causes an early transition to churn-turbulent flow when the superficial gas velocity is fixed at 0.83 cm/s. This has also been observed in a similar system with a different air injection method (Heindel and Monefeldt, 1997, 1998).

At a fibre concentration of C = 1% by mass, more, and larger, large bubbles are observed while the number of small bubbles has diminished (Fig. 2c). A fibre network begins to form at

this fibre concentration (Kerekes et al., 1985), and this can restrict bubble movement. A bubble can break through this network only if it is large enough (i.e., has a sufficient buoyant force). This results in considerable bubble coalescence. Bubble trains are also observed. For example, Fig. 2c shows three relatively large bubbles in the central column region. The lead bubble is pushing the fibre network away, creating a region of low fibre concentration in its wake. The trailing bubbles follow the lead bubble because of drag reduction, and they may even catch the lead bubble and coalesce with it. These bubbles still rise in a serpentine pattern but are generally confined to the central column region. This flow regime is also considered to be churn-turbulent.

At C = 1.5% by mass, the bubble rise patterns in Fig. 2d change slightly because the strength of the fibre network has increased. Instead of the main bubble flow oscillating back and forth in a serpentine pattern, the majority of the large bubbles rise in the central column region in an almost vertical path, creating a channel of low bubble rise resistance where other bubbles follow. Additionally, the channel location is not static due to the constant shifting of the fibre network caused by the rising bubbles. Small bubbles are still observed at this fibre concentration, but the number has decreased considerably. Also captured in Fig. 2d is a very large bubble with a much smaller bubble caught in its wake. These two bubbles are about to coalesce. Capturing this phenomena on film for an opaque suspension is one unique feature of the FXR technique.

Similar results are observed at C = 2% by mass (Fig. 2e). The fibre network strength also increases, causing the number of small bubbles to decrease while the size of the large bubbles increase.

When the fibre concentration is increased to C = 2.5% by mass (Fig. 2f), turbulent backmixing is no longer observed. Instead, the air bubbles rise in a nearly straight line in the

center of the column while a steady downward suspension movement is observed along the column sides. This movement appears in the column as two large and very slow-moving recirculation cells. The downward fibre movement also pushed the flexible air hose toward the column center. To prevent this and keep the sparger centrally located in the column, the hose was placed inside a small diameter pipe that was placed along the column wall (observed on the left-hand side of all radiographs with $C \geq 2.5\%$). This addition did not modify the downward slurry movement.

At a fibre mass of $C = 3\%$, Fig. 2g shows that the fibre network begins to hold some of the large bubbles in place for a period of time before other bubbles coalesce with them and/or the fibre network shifts to allow the trapped bubbles to rise. This results in some images with very few bubbles, while others like Fig. 2g having many large bubbles present with uncharacteristic bubble shapes. Although the gas flow regime still appears to be churn-turbulent with bubble coalescence and breakup freely occurring, the bubbles rise in surges where some are trapped and then expelled. Therefore, a more descriptive identification for this flow regime would be *surge churn-turbulent*.

Similar position 2 observations are recorded for $C = 3.5\%$ by mass in Fig. 2h. Additionally, at this concentration, the fibre network strengthens near the column base and appears to begin forming semi-rigid structures. This is caused by the rising bubbles carrying water-rich slurry to the surface, while fibre-rich slurry remains at the column base due to network interactions. Therefore, a fibre concentration gradient is created in the column where the overall fibre concentration is 3.5% by mass, but locally, the concentration is higher near the column base and lower near the column top. This causes a change in flow conditions at the column bottom (best observed in Fig. 3c). The fibre network is very dense on the column bottom

making it difficult for discrete air bubbles to rise through it. Discrete air channels are formed instead to allow the air to pass through the column bottom. The air channels are semi-static and remain active for periods of time ranging from a few seconds to a few minutes. Before a channel closes, another channel becomes active. Once the air channels reach a region in the bubble column that has a low enough local fibre concentration, individual air bubbles form. Hence, these channels are not observed in Fig. 2h for $C = 3.5\%$ by mass. The flow regime at the column base is defined as *discrete channel flow*, while surge churn-turbulent flow is still observed where discrete bubbles form.

As the fibre concentration increases to $C = 4$, 4.5, and 5% by mass (Figs. 2i, 2j, and 2k, respectively), the column region encompassing the discrete channel flow regime increases. The unusual flow pattern recorded at these fibre concentrations result from the periodic breakdown of the discrete channels. When this happens, a portion of the remaining air may become trapped and remain stationary until a new nearby channel forms.

Figure 3 displays composite overviews of the gas flow structures in the entire cellulose fibre suspension for four different fibre concentrations. Each FXR image was acquired at a separate time interval, and each column composite presents a qualitative picture of the gas flow (i.e., the dark regions in the FXR images). The air line is apparent on the left-hand side of each radiograph, and the central location of the sintered bronze sparger is schematically represented at the column base.

An air-water condition is again shown as a reference case (Fig. 3a). The vortical flow (Tzeng et al., 1993; Chen et al., 1994) is apparent throughout the column. The serpentine flow pattern is shown to start toward the right-hand side in position 1. The general upward gas flow

pattern oscillates from side to side, and the bubbles on the left-hand side of position 1 in Fig. 3a are caught in the backmixed flow. These bubbles eventually become entrained in the bulk upward air flow. Although bubble groupings are captured in the FXR images, little bubble coalescence or breakup is visually observed.

The column was initially charged to a fluid height of 80 cm. The air/fluid interface identified in position 4 is much higher than the original charge level due to the air bubbles in the system (i.e., gas holdup). The exact gas holdup value for these conditions is difficult to identify with a single radiograph of position 4 because the air/fluid interface fluctuates. Additionally, as shown in position 4 of Figs. 3a and 3b, the air/fluid interface is not smooth, but depends on the size of the bubbles breaking the surface. However, with a significant number of FXR images, average gas holdup could be recorded.

Churn-turbulent flow is shown in Fig. 3b for C = 0.5% by mass. The bubbles for this condition undergo frequent coalescence and breakup. In Fig. 3b, the serpentine flow pattern begins on the left-hand side of position 1 and small bubbles caught in the backmixed flow are recorded on the right-hand side of position 1. The spherical-capped bubbles are also readily captured in the radiographs. The deformation of the air/liquid interface as a result of two very large bubbles about to break the surface is also clearly evident in position 4 of Fig. 3b.

When C = 3.5% by mass (Fig. 3c), there appears to be a slight fibre concentration gradient in the bubble column, and the discrete channel gas flow regime is clearly visible at position 1. As the injected air rises, the discrete channels break down into individual bubbles when the local fibre concentration is low enough. As previously described, these bubbles may become trapped in the fibre network until other bubbles coalesce with them or disrupt the

network as they pass by, creating the surge churn-turbulent flow pattern. This results in the few bubbles captured in position 2 and many bubbles recorded in position 3.

At a fibre concentration of C = 5% by mass (Fig. 3d), discrete channel flow is observed throughout positions 1 and 2 and into position 3. The chaotic air bubble patterns are a result of the discrete air channels breaking down and reforming in different regions.

Although gas holdup was not measured in this study, it is apparent from the location of the air/liquid interface that it is similar when C = 0 and 0.5%, and it is reduced when C = 3.5%, and further reduced when C = 5% by mass. This reduction in gas holdup is consistent with other gas holdup studies in fibre suspensions (Lindsay et al. 1995; Reese et al., 1996; Janse et al. 1999).

CONCLUSIONS

Flash x-ray radiography was used to visualize gas flow structures in a bubble column filled with cellulose fibre suspensions at fibre concentrations as high as 5% by mass. It was shown that for a fixed superficial gas velocity of 0.83 cm/s, the gas flow regime in a fibre suspension changed from vortical to churn-turbulent when fibres were added to the bubble column. Two new flow regime descriptions were also identified at higher fibre concentrations. The first was defined as surge churn-turbulent flow, where churn-turbulent flow existed, but was observed as surges because the large bubbles were periodically trapped in the fibre suspension. The second new flow regime was identified as discrete channel flow, where individual channels of air form at the highest fibre concentrations.

ACKNOWLEDGMENTS

The assistance of Mr. Chris Ashley and Ms. Adele Garner with the FXR images is greatly appreciated. Support by the Undergraduate Summer Intern Program at the Institute of Paper Science and Technology through IPST and its Member Companies is also gratefully acknowledged.

REFERENCES

Bennett, A.W., G.F. Hewitt, H.A. Kearsey, R.K.F. Keeys and P.M.C. Lacey, "Flow Visualization Studies of Boiling at High Pressure", Proc. Inst. Mech. Eng., Part 3C **180**, 1-11 (1965).

Cartz, L., "Nondestructive Testing", ASM International, Materials Park, OH (1995).

Chen, R.C., J. Reese and L.-S. Fan, "Flow Structure in a Three-Dimensional Bubble Column and Three-Phase Fluidised Bed", AIChE J. **40**, No. 7, 1093-1104 (1994).

De Swart, J.W.A., R.E. Van Vliet and R. Krishna, "Size, Structure and Dynamics of 'Large' Bubbles in a Two-Dimensional Slurry Bubble Column", Chem. Eng. Sci. **51**, No. 20, 4619-4629 (1996).

Heindel, T.J., "Bubble Size Measurements in a Fibre Suspension", J. Pulp Pap. Sci. **25**, No. 3, 104-110 (1999).

Heindel, T.J. and A.E. Garner, "The Effect of Fibre Consistency on Bubble Size", Nord. Pulp Pap. Res. J. **14**, No. 2, 171-178 (1999).

Heindel, T.J. and J.L. Monefeldt, "Flash X-ray Radiography for Visualizing Gas Flows in Opaque Liquid/Fibre Suspensions," in "6th International Symposium on Gas-Liquid Two-Phase Flows", Vancouver, BC, June 22-26, 1997, ASME Press, New York (1997), Paper FEDSM97-3526.

Heindel, T.J. and J.L. Monefeldt, "Observations of the Bubble Dynamics in a Pulp Suspension Using Flash X-ray Radiography", TAPPI J. **81**, No. 11, 149-158 (1998).

Hewitt, G.F., "Measurement of Two Phase Flow Parameters", Academic Press, New York (1978).

Hewitt, G.F., "Flow Regimes", in "Handbook of Multiphase Systems", G. Hetsroni, Ed., Hemisphere Publishing Corp., New York (1982), Chapter 2.1.

Hewitt, G.F. and D.N. Roberts, "Studies of Two-Phase Flow Patterns by Simultaneous X-ray and Flash Photography", United Kingdom Atomic Energy Authority (UKAEA), Harwell, Berkshire (1969), Report Number: AERE-M2159.

Jamet, F. and G. Thomer, "Flash Radiography", Elsevier Publishing Company, Inc., New York (1976).

Janse, P., C.O. Gomez and J.A. Finch, "Effect of Pulp Fibres on Gas Holdup in a Flotation Column", Can. J. Chem. Eng. **77**, 22-25 (1999).

Kerekes, R.J., R.M. Soszynski and P.A. Tam Doo, "The Flocculation of Pulp Fibres", in "Papermaking Raw Materials", V. Punton, Ed., Mechanical Engineering Publications Limited, London (1985), pp. 265-310.

Kumar, S.B., D. Moslemian and M.P. Dudukovic, "Gas-Holdup Measurements in Bubble Columns Using Computed Tomography", AIChE J. **43**, No. 6, 1414-1425 (1997).

Letzel, H.M., J.C. Schouten, R. Krishna and C.M. van den Bleek, "Characterization of Regimes and Regime Transitions in Bubble Columns by Chaos Analysis of Pressure Signals", Chem. Eng. Sci. **52**, No. 24, 4447-4459 (1997).

Lindsay, J.D., S.M. Ghiaasiaan and S.I. Abdel-Khalik, "Macroscopic Flow Structure in a Bubbling Paper Pulp-Water Slurry", Ind. Eng. Chem. Res. **34**, 3342-3354 (1995).

Reese, J., P. Jiang and L.-S. Fan, "Bubble Characteristics in Three-Phase Systems Used for Pulp and Paper Processing", Chem. Eng. Sci. **51**, No. 10, 2501-2510 (1996).

Rowe, P.N. and B.A. Partridge, "An X-ray Study of Bubbles in Fluidised Beds", Trans. Inst. Chem. Eng. **43**, T157-T175 (1965).

Sarrafi, A., M. Jamialahmadi, H. Müller-Steinhagen and J.M. Smith, "Gas Holdup in Homogeneous and Heterogeneous Gas-Liquid Bubble Column Reactors", Can. J. Chem. Eng. 77, 11-21 (1999).

Saxena, S.C., D. Patel, D.N. Smith and J.A. Ruether, "An Assessment of Experimental Techniques for the Measurement of Bubble Size in a Bubble Slurry Reactor as Applied to Indirect Coal Liquefaction", Chem. Eng. Comm. **63**, 87-127 (1988).

Shollenberger, K.A., J.R. Torczynski, D.R. Adkins, T.J. O'Hern and N.B. Jackson, "Gamma-Densitometry Tomography of Gas Holdup Spatial Distribution in Industrial-Scale Bubble Columns", Chem. Eng. Sci. **52**, No. 13, 2037-2048 (1997).

Tsuchiya, K., K. Ohsaki and K. Taguchi, "Large and Small Bubble Interaction Patterns in a Bubble Column", Int. J. Multiphase Flow **22**, No. 1, 121-132 (1996).

Tzeng, J.-W., R.C. Chen and L.-S. Fan, "Visualization of Flow Characteristics in a 2-D Bubble Column and Three-Phase Fluidized Bed", AIChE J. **39**, No. 5, 733-744 (1993).

Zahradnik, J., M. Fialova, M. Ruzicka, J. Drahos, F. Kastanek and N.H. Thomas, "Duality of the Gas-Liquid Flow Regimes in Bubble Column Reactors", Chem. Eng. Sci. **52**, No. 21/22, 3811-3826 (1997).

Zhang, J.-P., J.R. Grace, N. Epstein and K.S. Lim, "Flow Regime Identification in Gas-Liquid Flow and Three-Phase Fluidized Beds", Chem. Eng. Sci. **52**, No. 21/22, 3979-3992 (1997).

LIST OF FIGURES

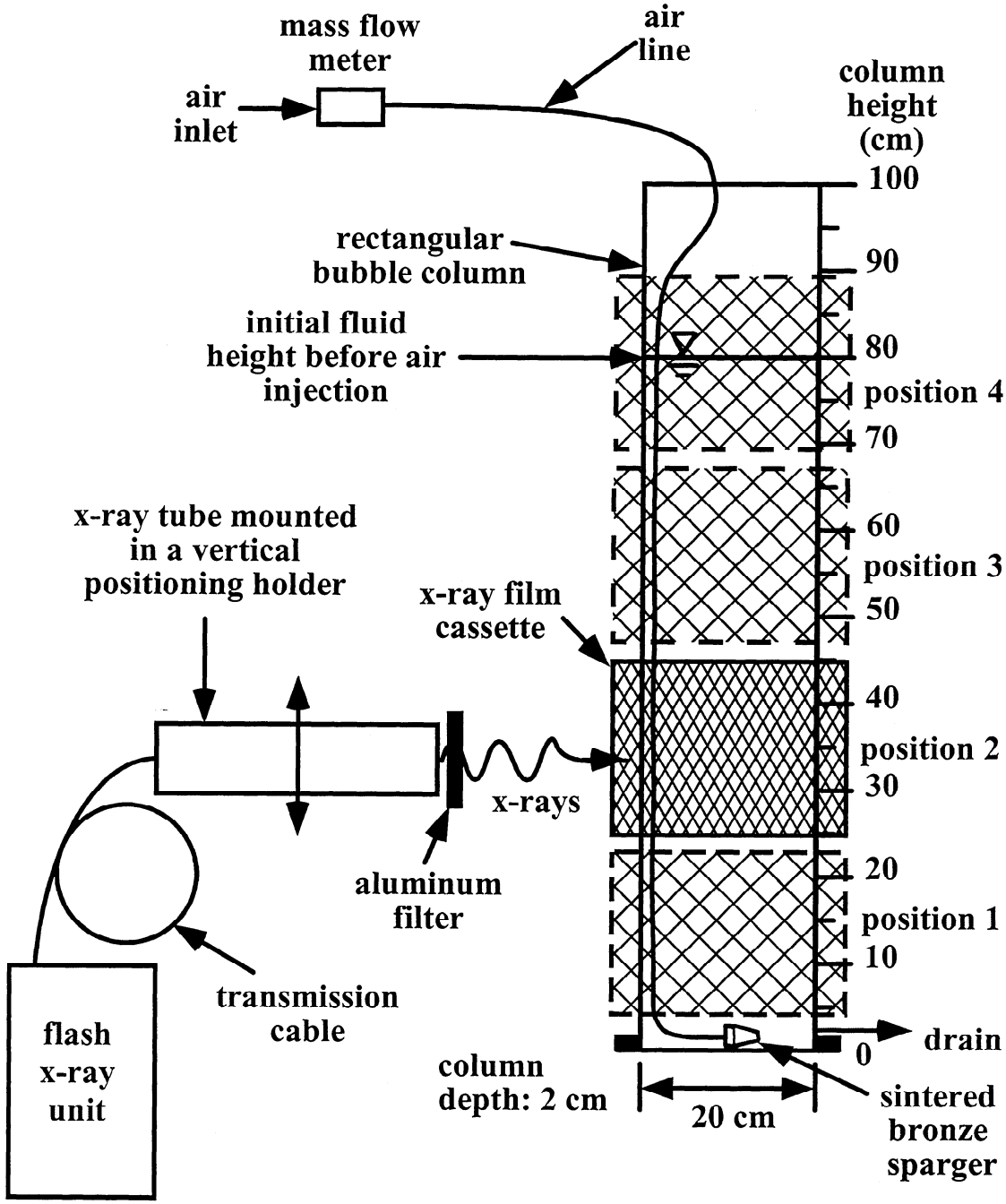

MS # 7919N Figure 1

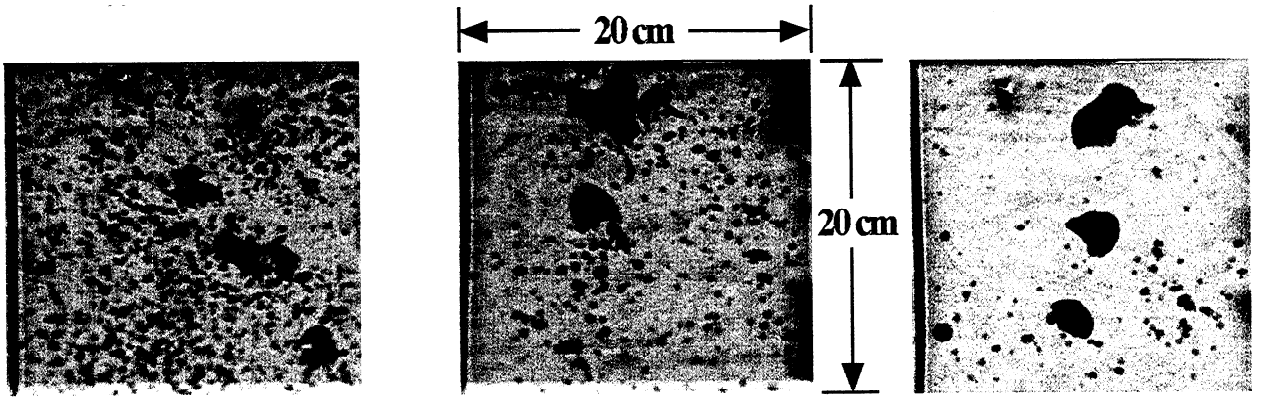

(a) $C = 0\%$ (b) $C = 0.5\%$ (c) $C = 1\%$

(d) $C = 1.5\%$ (e) $C = 2\%$ (f) $C = 2.5\%$

(g) $C = 3\%$ (h) $C = 3.5\%$ (i) $C = 4\%$

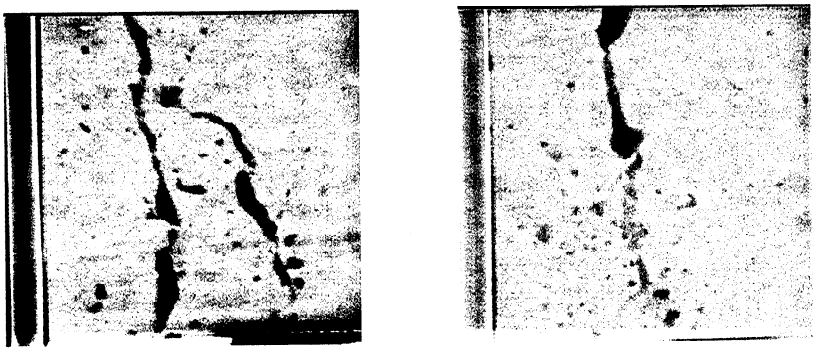

(j) $C = 4.5\%$ (k) $C = 5\%$

MS # 7919N Figure 2

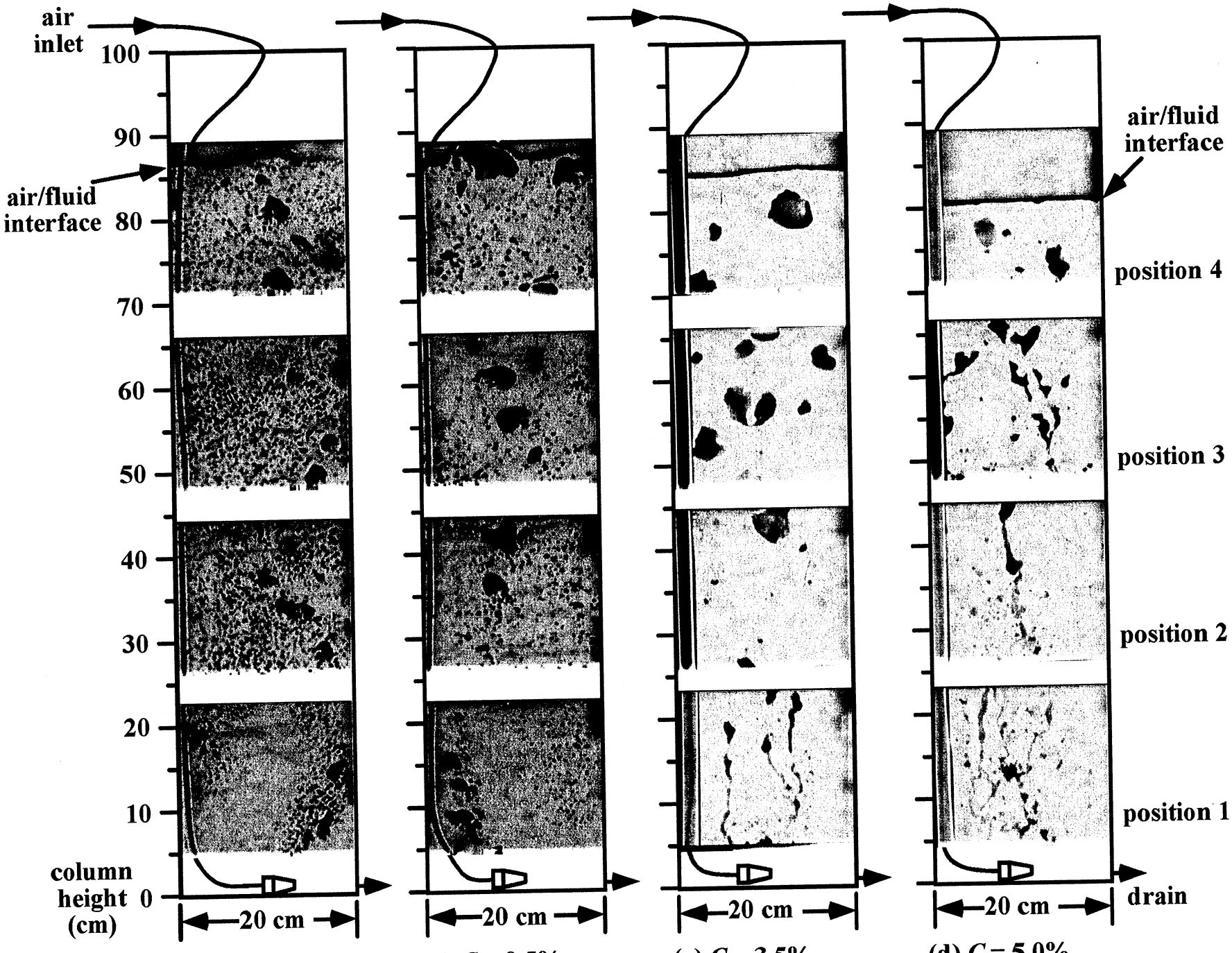

MS # 7919N Figure 3